Evolution of entanglement entropy in the D1-D5 brane system

Curtis T. Asplund and Steven G. Avery

Phys. Rev. D **84**, 124053 — Published 27 December 2011

DOI: 10.1103/PhysRevD.84.124053

NSF-KITP-11-179
IMSc/2011/8/7

Evolution of entanglement entropy in the D1–D5 brane system

Curtis T. Asplund[1,*] and Steven G. Avery[2,3,†]

[1]*Department of Physics, University of California, Santa Barbara, CA 93106*

[2]*The Institute of Mathematical Sciences, CIT Campus, Taramani, Chennai, India 600113*

[3]*Kavli Institute for Theoretical Physics, University of California, Santa Barbara, CA 93106, USA*

We calculate the evolution of the geometric entanglement entropy following a local quench in the D1D5 conformal field theory, a two-dimensional theory that describes a particular bound state of D1 and D5 branes. The quench corresponds to a localized insertion of the exactly marginal operator that deforms the field theory off of the orbifold (free) point in its moduli space. This deformation ultimately leads to thermalization of the system. We find an exact analytic expression for the entanglement entropy of any spatial interval as a function of time after the quench and analyze its properties. This process is holographically dual to one stage in the formation of a stringy black hole.

I. INTRODUCTION

Consider an initial, smooth configuration of matter that collapses into a black hole. There are longstanding questions about how the information in the initial configuration, such as the entanglement between various subsystems, becomes encoded in the resulting black hole. As a quantum theory of gravity, string theory addresses many of these questions. While the AdS/CFT correspondence leads immediately to the proposal that certain black holes are dual to thermal mixed states of a dual conformal field theory (CFT) [1], this says little about the formation process. To go further toward answering such dynamical questions, one needs to study the unitary evolution of a CFT with a gravitational dual, undergoing thermalization. In this paper we begin such an investigation in the D1D5 CFT, which describes a bound state of D1 and D5 branes, and is well-known as a useful system for studying black holes in string theory.

* casplund@physics.ucsb.edu

† avery@mps.ohio-state.edu

We study this process using the entanglement entropy, defined below, which measures entanglement between subsystems in a quantum system. As opposed to the many studies of black hole entropy as entanglement entropy of different parts of the bulk spacetime or between different boundary CFTs ([2] reviews many of these), we are considering the evolution of the entanglement entropy of subsystems of a single CFT, in order to study its thermalization. The connection between quantum entanglement and thermodynamics has a long history. See [3] for a short review, [4, 5] for relevant early investigations and [6–10] for recent general results.

As a brief review, begin with a quantum system with Hilbert space $\mathcal{H}$ and Hamiltonian H. Then factorize, or coarse-grain, the Hilbert space of the full system as $\mathcal{H} = \mathcal{H}_A \otimes \mathcal{H}_E$, where the first factor contains all states describing degrees of freedom in a subsystem A and the second factor all states for the exterior of A—the "environment" E. We call a quantum system, in a state specified by a density matrix ρ, thermalized if for general small subsystems A the reduced density matrices ρ_A, obtained by tracing over $\mathcal{H}_E$, are approximately (Gibbs/canonical ensemble) thermal mixed states, e.g.,

$$\rho_A \approx \frac{e^{-\beta H_A}}{Z_A} \tag{1.1}$$

for some β (the inverse temperature), where $H_A = \mathrm{Tr}_E\, H$ and $Z_A = \mathrm{Tr}_A\, e^{-\beta H_A}$. This is an admittedly imprecise definition of "thermalized," but is sufficient for our purposes. The expression in (1.1) is appropriate for those cases where the Hamiltonian is the only conserved quantity. For systems with more symmetries, including integrable systems with infinitely many conserved quantities, one can still define generalized Gibbs ensembles and appropriate thermal reduced density matrices, characterized by generalized chemical potentials in addition to β [6, 8]. This is relevant for CFTs like the one we consider, which undergo a quench but which subsequently evolve as free theories and are characterized by a set of momentum-dependent temperatures [10, 11].

We are concerned here with the case that the full system AE is in a pure state, i.e., a closed quantum system. Then the fact that ρ_A is mixed comes entirely from the entanglement of A with E. This entanglement can be measured in a variety of ways, but in this paper we consider the Rényi and von Neumann entropies, which are given by (3.3) below. We choose these quantities for a number of reasons, including nice analytic properties and calculability, to be discussed in the paper. Here we just emphasize that they let one track the thermalization of various subsystems as well as deviations from strictly thermal behavior (see [12] §8.2 for an introductory discussion of this topic). The entanglement entropies, as a function of subsystem, time, and other parameters, can also yield much other information about the system. This is explored in voluminous recent work in condensed matter physics (see [13] for several recent reviews).

One can use these quantities, in principle, to investigate the recently conjectured thermalization time for black holes that saturates a causality bound [14], although we don't get that far in this paper. As we discuss below, it is technically difficult to quantitatively compare the non-equilibrium dynamics we study here to the system in equilibrium and the full thermalization process. However, we can still learn a lot from the results we present.

Motivated by the rapid thermalization observed in heavy ion collisions as well as the theoretical questions already mentioned, there are many investigations that use AdS/CFT to study strongly-coupled CFTs far from equilibrium or undergoing thermalization, e.g., [15–21]. Some of these [22–25] also use entanglement entropy via the holographic entanglement entropy proposal [26, 27] (see also [28] for a recent study of the holographic Rényi entropies). These latter investigations use the dual classical geometry and so cannot address some of the most puzzling questions about information in black holes, which involve quantum mechanics of the bulk theory in an essential way.

We study the D1D5 CFT at weak coupling, which has long been used in string theory to study black holes [29, 30]. Early studies focused on the extremal, zero-temperature configurations, whereas we consider exciting to a state that is far from extremal. Recent work has studied Hawking radiation in this system in detail [31–35] and deformations of the CFT away from the orbifold (free) point in the moduli space [36–38] (see also [39, 40] for leading order calculations away from the orbifold point). Because we work at weak coupling, i.e. near the orbifold point, we are not in the regime where supergravity is a good approximation. Nonetheless the above work indicates that this regime contains much information about black holes. Additional support for this includes several precise matchings between gravitational calculations and calculations from the free theory data [41–43]. More evidence for the surprising efficacy of the orbifold CFT in describing black holes comes from the very recent paper [44]. There are also general arguments for thermalization of CFTs with gravity duals in the large N limit at any finite value of the coupling [45] corroborated by exact calculations in simplified models [46, 47]. The resulting weakly-coupled thermal state is dual to a "stringy black hole," in that the string length is large compared to the size of the black hole (see [45] for further discussion of stringy black holes). The above work indicates that such a state should also tell us about traditional black holes.

In particular, the results illustrated in §VI have a natural explanation in terms of free excitations traveling at the speed of light around the S^1. This picture is similar to the CFT description in [48, 49] of near-extremal supergravity excitations, which, when the decoupling limit is relaxed, can periodically escape the AdS throat to the asymptotic flat space. The period and rate of emission were reproduced from the same kind of CFT dynamics we observe. Thus our results correctly capture some qualitative aspects of the supergravity description. On the other hand, we expect that large energy (far from extremal) supergravity excitations can back-react to form black holes. In the CFT, this corresponds to thermalization. Since the entanglement entropy that we find does not persist, but rather has short-time periodic dynamics, we conclude that, as expected, the orbifold CFT does not capture this important process. We hope to address this issue more quantitatively in future works.

A closely related precursor to our work is [50], which also calculates the evolution of entanglement entropy in a weakly-coupled CFT. They proposed this as a way to study quantum black hole formation and emphasized that the entanglement entropy can be thought of as a coarse-grained thermodynamic entropy. However, their CFT (a single fermion) has no clear dual black hole interpretation, although it does illustrate some general features of the kind of problem we are considering.

The general process of thermalization in weakly coupled theories is well-studied, but the D1D5 system exhibits some novel features. In particular, we consider dynamics arising from a localized insertion of a particular marginal deformation of the orbifold CFT that acts as a *local quench*, to be described below. The calculation of the entropy produced by this quench is the main result of this paper. This is the basic process by which entropy is generated.

As emphasized in [45], the familiar semi-classical dynamics of black holes, including the puzzling apparent loss of information, should appear in the limit $N \to \infty$ of the dual holographic theory. Here that would correspond to the limit of infinitely many D1 and D5 branes. We do not consider that limit here, rather we consider a finite number of branes unitarily evolving toward a thermalized pure state as described above. In this paper we just analyze the basic process in that evolution.

In §II we review the D1D5 CFT and the marginal deformations that we study. In §III we set up the calculation of the entanglement entropies in the CFT, including a review of the replica trick. Next, in §IV we compute the four-point function that we need to calculate the entropies, which we do in §V. We illustrate some of their properties in §VI. We conclude with a discussion of our results and future directions.

II. D1D5 REVIEW

The D1D5 system is realized in IIB string theory compactified on[1] $T^4 \times S^1$ with the bound state of N_1 D1-branes wrapping the S^1 and N_5 D5-branes wrapping $T^4 \times S^1$. We take the S^1 to be large compared to the T^4. The near-horizon limit of the geometry is $AdS_3 \times S^3 \times T^4$, which is dual to a two-dimensional CFT living on the boundary of AdS_3.

The two-dimensional D1D5 CFT has $\mathcal{N} = (4,4)$ supersymmetry with $\mathrm{SU}(2)_L \times \mathrm{SU}(2)_R$ R-symmetry corresponding to the isometry of the S^3. The two-dimensional base space of the CFT is given by the cylindrical boundary of AdS_3 parametrized by time and the S^1. In addition, we can organize the field content using the $\mathrm{SO}(4)_I \simeq \mathrm{SU}(2)_1 \times \mathrm{SU}(2)_2$ symmetry broken by the compactification on T^4. One can also fix the total central charge $c = 6N_1N_5$ from the algebra of diffeomorphisms that preserve the asymptotic AdS_3. The CFT has a twenty-dimensional moduli space that corresponds to the near-horizon twenty-dimensional moduli space of the IIB supergravity compactification.

There is a point in moduli space called the "orbifold point," analogous to free super Yang-Mills theory in $\mathrm{AdS}_5/\mathrm{CFT}_4$, where the D1D5 CFT is a sigma model with orbifolded target space, $(T^4)^{N_1N_5}/S_{N_1N_5}$. Just as the dual of free super Yang-Mills theory does not have a geometric description, the orbifold CFT is far from points in moduli space that are well described by supergravity. We wish to study the effect of certain $(4,4)$ exactly marginal deformations that move the orbifold CFT toward points in moduli space that should have geometric descriptions and, in particular, should include black hole physics. Even though we work far from the supergravity regime, as discussed in the introduction,

[1] One may also consider K3 instead of T^4.

we can still capture some black hole physics.

We can think of the orbifold model as N_1N_5 copies of a $(4,4)$ $c=6$ CFT. Each copy has four real bosons that are vectors of SO$(4)_I$, X^i, and their fermionic superpartners. See, e.g., [51] for details. For computational purposes, we map the real cylinder coordinates, $t \in \mathbb{R}$ and $y \in [0, 2\pi R)$, to dimensionless complex coordinates on the cylinder

$$w = \tau + i\sigma \qquad \frac{t}{R} \mapsto -i\tau \qquad \frac{y}{R} = \theta. \tag{2.1}$$

Note that we have also incorporated a Wick rotation in this step. We prefer to perform most of the computation in the complex plane by further mapping to coordinates

$$z = e^{w} \qquad \bar{z} = e^{\bar{w}}. \tag{2.2}$$

In addition to the local bosonic and fermionic excitations of each copy, the orbifold theory also has twisted sectors: states which come back to themselves only up to an element of the orbifold group $S_{N_1N_5}$ upon circling the S^1. The twist operators $\sigma_n(z)$ are labeled by n-cycles and change the twist sector of the theory. More concretely, consider operators $O^{(i)}(z)$ in the ith copy. In the presence of $\sigma_{(12\ldots n)}(z_0)$, the operators have boundary conditions

$$O^{(i)}(z_0 + ze^{2\pi i}) = \begin{cases} O^{(i+1)}(z_0+z) & i = 1, \ldots, n-1 \\ O^{(1)}(z_0+z) & i = n \\ O^{(i)}(z_0+z) & i = n+1, \ldots, N_1N_5 \end{cases} . \tag{2.3}$$

Let us emphasize that the twist operators considered here are physical components of the orbifold CFT, and should not be confused with twist operators introduced as part of the replica trick.

Following [36–38], we focus on four of the marginal deformations that involve twist operators. These operators are believed to be responsible for thermalization in the D1D5 CFT. The $(4,4)$ supersymmetric deformations are singlets under SU$(2)_L \times$ SU$(2)_R$. To obtain such a singlet we apply modes of the supercharges $G^{\mp}_{\dot{A}}$ to $\sigma_2^{\pm}$, where we use plus/minus indices to label elements of SU$(2)_L$ doublets and dotted capital Latin indices for doublets of SU$(2)_2$. In [36] it was shown that we can write the deformation operator(s) as

$$\widehat{O}_{\dot{A}\dot{B}}(w_0) = 2\Big[\int_{w_0} \frac{\mathrm{d}w}{2\pi i} G^{-}_{\dot{A}}(w)\Big]\Big[\int_{\bar{w}_0} \frac{\mathrm{d}\bar{w}}{2\pi i} \bar{G}^{-}_{\dot{B}}(\bar{w})\Big]\sigma_2^{++}(w_0), \tag{2.4}$$

where the factor of 2 normalizes the operator. The operator σ_2^+ is normalized to have unit OPE with its conjugate

$$\sigma_{2,+}(z')\sigma_2^+(z) \sim \frac{1}{z'-z}. \tag{2.5}$$

This implies that acting on the Ramond vacuum [36]

$$\sigma_2^+(z)|0_R^-\rangle^{(1)}|0_R^-\rangle^{(2)} = |0_R^-\rangle + O(z). \tag{2.6}$$

Here $|0_R^-\rangle$ is the spin down Ramond vacuum of the CFT on the doubly wound circle produced after the twist. The normalization (2.6) has given us the coefficient unity for the first term on the RHS and the $O(z)$ represent excited states of the CFT on the doubly wound circle.

III. SET UP

Let us now outline the precise calculation we perform. Since we are interested in the dynamics of thermalization or scrambling in the CFT, we quench the system and then look at the entanglement entropy of spatial subsystems as a function of time. The entanglement entropy of subsystems, as discussed, is a very natural quantity to examine when discussing thermalization. Happily, there is already some considerable technology for computing the entanglement entropy after both global and local quenches in two-dimensional CFTs [52, 53].

The specific quench we consider is a local insertion of the deformation operator introduced above. Since this operator is believed to be responsible for thermalization, it seems natural to consider the dynamics after its application. Moreover, these results should tie in strongly with previous investigations [36–38], which showed that the deformation operator, in essence, effects a Bogolyubov transformation. For instance, the deformation operator, when acting on the vacuum, produces a squeezed state of the form [36]

$$\sigma_2^+(z_0)\,|0_R^-\rangle^{(1)}\,|0_R^-\rangle^{(2)} = \exp\left[-\frac{1}{2}\sum_{m,n}\gamma^B_{mn}\alpha_{A\dot{A},-m}\alpha^{A\dot{A}}_{-n} + \sum_{m,n}\gamma^F_{mn}\psi^{+A}_{-m}\psi^{-}{}_{A,-n}\right]|0_R^-\rangle\,. \tag{3.1}$$

In this equation, we only show the left (holomorphic) sector and consider just the twist part of the deformation. On the left-hand side we have the two-twist operator acting on the untwisted Ramond vacua, which produces many pairs of bosonic and fermionic excitations on the two-twisted Ramond vacuum. Note that the Ramond vacua have an $\mathrm{SU}(2)_L \times \mathrm{SU}(2)_R$ spin structure. The coefficients γ^B and γ^F are functions of z_0 given explicitly in [36]. The calculation we propose, then, computes the time dependence of the entanglement entropy of this squeezed state; although, we do not use the above form explicitly.

The physical setup is as follows. We apply the deformation operator (2.4) to the Ramond vacuum at time $t = 0$ and $y = 0$. We then look at the time-dependence of the entanglement entropy of an arbitrary spatial interval. Since we are mostly interested in how the entanglement entropy changes due to the quench, we subtract off the entanglement entropy of the vacuum. We act in the Ramond sector since that is the sector relevant for black holes. We will sketch the gravitational picture this corresponds to in the final section.

III.1. Review of the replica trick for computing entanglement entropy

In the remainder of this section, we set up the calculation of the entanglement entropy after the quench. Consider a system S with some subsystem A, and its complement B. Recall that the (von Neumann) entanglement entropy of A in S is defined as the von Neumann entropy of the reduced density matrix,

$$S(A) = -\operatorname{Tr}_A \hat{\rho}_A \log \hat{\rho}_A \qquad \hat{\rho}_A = \operatorname{Tr}_B \hat{\rho}_S. \tag{3.2}$$

The density matrix $\hat{\rho}_S$ is the density matrix for the full system S. If, as is true throughout this paper, the total system S is in a pure state $|\psi\rangle$, then $\hat{\rho}_S = |\psi\rangle\langle\psi|$. For our calculation, the subsystem A corresponds to degrees of freedom living on some interval of S^1. This definition has a number of nice properties that make it the natural measure of entanglement including positive definiteness, strong subadditivity, and $S(A) = S(B)$ for a pure state. In fact, this is essentially the unique measure of entanglement satisfying the above properties [54].

Computing the von Neumann entanglement entropy is computationally difficult because of the log, so instead we follow [55–57] and use the replica trick: we first compute the Rényi entropy of order n and then analytically continue to the von Neumann entropy.

Recall that the Rényi entropy of order n is defined as

$$S_n(A) = \frac{1}{1-n} \log\left(\mathrm{Tr}_A\, \hat{\rho}_A^n\right) \quad \text{and} \quad S_{\mathrm{vN}}(A) = \lim_{n\to 1} S_n(A). \tag{3.3}$$

The Rényi entropies are an interesting measure of entanglement even before taking the limit to the von Neumann entanglement entropy. In particular, they serve as a lower bound on S_{vN} and vanish on an unentangled state.

Before showing how to compute the Rényi entropy, we first review how to write the density matrix $\hat{\rho}_S$ as a path integral. From there we can easily compute $\mathrm{Tr}\,\rho_A^n$ as a path integral with twisted boundary conditions. Let us work in some basis with states that we will write as $|\varphi\rangle$; it is perhaps most natural to think of these as shape states (field eigenstates), but any basis works. Then, the φ_1–φ_2 element of the density matrix at time T can be written as

$$\begin{aligned} \langle\varphi_2|\, \hat{\rho}(T)\, |\varphi_1\rangle &= \langle\varphi_2|\psi(T)\rangle \langle\psi(T)|\varphi_1\rangle \\ &= \langle\varphi_2|\, e^{-i\hat{H}T}\, |\psi_0\rangle \langle\psi_0|\, e^{i\hat{H}T}\, |\varphi_1\rangle \\ &= \langle\psi_0|\, e^{i\hat{H}T}\, |\varphi_1\rangle \langle\varphi_2|\, e^{-i\hat{H}T}\, |\psi_0\rangle\,, \end{aligned} \tag{3.4}$$

where we have suggestively switched the order of the two amplitudes for reasons that should become clear. The state $|\psi_0\rangle$ is the state at $t = 0$, which for us is the state immediately after the quench. We have the product of two amplitudes, each of which can be written as a separate path integral; however, it is more fruitful to think of this as one path integral with discontinuous intermediate boundary conditions. More specifically,

$$\begin{aligned} \langle\varphi_2|\, \hat{\rho}(T)\, |\varphi_1\rangle &= \int D\phi(t)\Big|_{\phi(-T)=\psi_0}^{\phi(0)=\varphi_2} e^{i\int_{-T}^{0} \mathrm{d}t\, L(\phi(t))} \int D\phi(t)\Big|_{\phi(0)=\varphi_1}^{\phi(-T)=\psi_0} e^{i\int_{0}^{-T} \mathrm{d}t\, L(\phi(t))} \\ &= \int D\phi(t)\Big|_{\mathrm{BCs}} e^{i\int_C \mathrm{d}t\, L(\phi(t))}, \end{aligned} \tag{3.5}$$

where "BCs" in the last line indicates the boundary conditions from the previous line, and the contour C starts at $t = -T$ goes to $t = 0$ and then backwards to $t = -T$. We see, then, that we can think of the density matrix as a path integral which accepts two boundary conditions at $t = 0$. We have translated the ψ_0 boundary condition down to $t = -T$ to match with previous calculations [52, 53].

While this is formally correct, there are a couple of subtleties to address. First of all, we should clarify what we mean by the above path integral, since as written we need double-valued fields. It is more precise to parametrize C as

$$t = \begin{cases} s & s \in [-T, 0] \\ -s & s \in (0, T] \end{cases} \qquad s \in [-T, T], \tag{3.6}$$

in which case the action in the path integral becomes

$$\int_C \mathrm{d}t\, L(\phi(t)) = \int_{-T}^{0} \mathrm{d}s\, L(\phi(s)) - \int_0^T \mathrm{d}s\, L^T(\phi(s)), \tag{3.7}$$

and ϕ is single-valued on s. We put the superscipt T on L in the second term to indicate that it is the time-reversed Lagrangian. The second issue we need to address is Wick-rotating the path integral. We usually Wick-rotate the path integral to imaginary time to make the oscillatory term iS into a convergent $-S_E$; however, we now have a minus sign between the two terms in (3.7), which means that we should Wick-rotate the two terms oppositely. When we Wick-rotate the second part in the opposite direction, we get rid of the minus sign and the time-reversal: we get a smoothly defined Euclidean path integral

$$\begin{aligned} &Z(\tau_0, \tau_f; \psi_0; \varphi_1, \varphi_2) = \int D\phi(\tau)\Big|_{\text{BCs}} \exp\left(-\int_{\tau_0}^{\tau_f} \mathrm{d}\tau\, L_E(\phi(\tau))\right) \\ &\text{BCs:} \quad \phi(\tau_0) = \phi(\tau_f) = \psi_0, \qquad \phi(0^-) = \varphi_2, \qquad \phi(0^+) = \varphi_1. \end{aligned} \tag{3.8}$$

We can compute this path integral for $\tau_0 < 0 < \tau_f$ with real τ_0 and τ_f, and finally analyt-

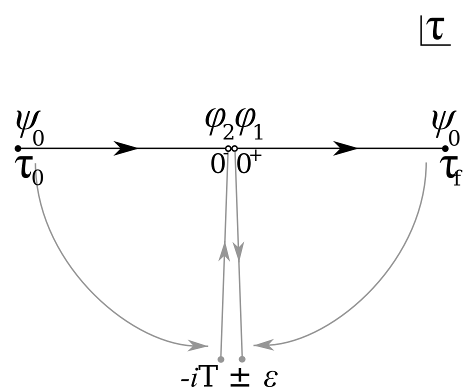

FIG. 1. The contour along the real axis of the complex τ-plane for the Euclidean path integral. The analytic continuation back to Lorentzian time is shown in light gray, which shows how the ϵ regularization arises.

ically continue to the desired matrix element via

$$\langle \varphi_2 |\, \hat{\rho}\, | \varphi_1 \rangle = \lim_{\epsilon \to 0^+} N_\epsilon\, Z(-iT - \epsilon, -iT + \epsilon; \psi_0; \varphi_1, \varphi_2), \tag{3.9}$$

where we put in ϵ to "remember" which direction we Wick-rotated the two terms. The factor of N_ϵ is a normalization constant that ensures $\operatorname{Tr}\hat{\rho} = 1$,

$$\frac{1}{N_\epsilon} = \langle\psi_0| e^{-(2\epsilon)\hat{H}} |\psi_0\rangle = \int D\varphi \, Z(-iT - \epsilon, -iT + \epsilon; \psi_0; \varphi, \varphi). \tag{3.10}$$

The limit as $\epsilon \to 0$ is both delicate and crucial to getting the right physics, since $\phi(\tau)$ has a branch cut along the negative imaginary axis. Later, it should become clear that ϵ plays the role of a UV cutoff.

Before continuing, let us remark that the above should be reminiscent of the Schwinger–Keldysh, or closed time path, formalism with temperature $T = 1/(2\epsilon)$ (see, e.g., [58] for a review of this formalism). Indeed, if one integrates over ψ_0, then it is exactly the Schwinger–Keldysh formalism, with some insertions at $t = 0$. Also note that if one identifies $\varphi_1 = \varphi_2 = \varphi$ and integrates over φ, then one computes $\operatorname{Tr}\hat{\rho}$, which is unity for a pure state.

We now have all of the tools to understand how to compute the Rényi entanglement entropy as a function of time after the quench. First note that it should now be clear how to compute the reduced density matrix (3.2):

$$\begin{aligned}
\langle a_2| \hat{\rho}_A |a_1\rangle &= \langle a_2| \operatorname{Tr}_B \hat{\rho} \, |a_1\rangle \\
&= \int_B Db \, N_\epsilon Z\big(-iT - \epsilon, -iT + \epsilon; \psi_0; \varphi_1 = \{a_1, b\}, \varphi_2 = \{a_2, b\}\big) \\
&\equiv N_\epsilon Z_A\big(-iT - \epsilon, -iT + \epsilon; \psi_0; a_1, a_2\big).
\end{aligned} \tag{3.11}$$

Here we indicate a field taking values a on A and b on B by $\{a, b\}$. We can compute this quantity from the same path integral in (3.8) with altered boundary conditions at $t = 0$. In the region B, we now demand that ϕ be continuous at $t = 0$. We started with a full cut, which we sew together in region B. The boundary conditions on the remainder determine the matrix element computed. This manifold is pictured in Figure 2.

Now, to compute $\operatorname{Tr}_A \hat{\rho}_A^n$ we start by inserting $\int Da \, |a\rangle \langle a|$ in between each $\hat{\rho}_A$ and then perform the trace in the $|a\rangle$ basis. This becomes n distinct copies of the above path integral with appropriate integrals over the a_i:

$$\begin{aligned}
\operatorname{Tr}\hat{\rho}_A^n &= \int Da_0 \int Da_1 \cdots \int Da_{n-1} \; \langle a_0| \hat{\rho}_A |a_{n-1}\rangle \cdots \langle a_2| \hat{\rho}_A |a_1\rangle \langle a_1| \hat{\rho}_A |a_0\rangle \\
&= \int Da_0 \cdots \int Da_{n-1} (N_\epsilon)^n \; Z_A(\tau_0, \tau_f; \psi_0; a_{n-1}, a_0) \cdots Z_A(\tau_0, \tau_f; \psi_0; a_0, a_1),
\end{aligned} \tag{3.12}$$

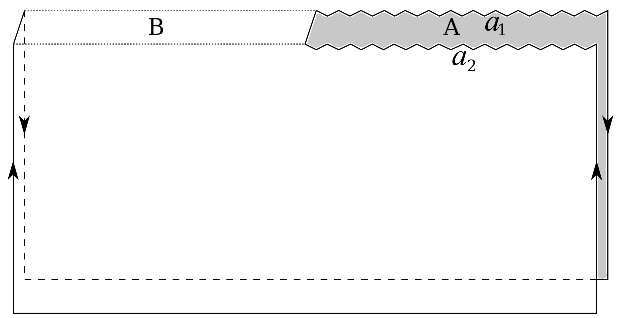

FIG. 2. The reduced density matrix as a path integral. Note that flat piece on top is there for illustrative purposes only. The boundary condition on the bottom two edges are both $|\psi_0\rangle$; whereas, the boundaries in region A are "inputs" which determine the matrix element of the reduced density matrix.

where τ_0 and τ_f get analytically continued as described. One can then put all of the pieces into a single path integral over n replicas, with n-twisted boundary conditions in region A connecting the replicas and singly-twisted boundary conditions outside of A.

III.2. Entanglement entropy in the D1D5 CFT

Let us apply the above general discussion to the matter at hand. We need to compute the twisted path integral described above. We can rewrite the path integral as a correlator of local twist operators that induce the appropriate monodromy, and then compute the correlator using techniques in [59]. Let us note that there is an extra layer of obfuscation beyond computations in other CFTs since our quench involves a distinct twist operator that is part of the physical spectrum of the CFT.

We prepare the state $|\psi_0\rangle$ by starting with the vacuum at $\tau = -\infty$, evolving forward to τ_0 where we insert our quench $\widehat{O}(w_0)$ from (2.4). To compute the Rényi entropy, we need n replicas of $|\psi_0\rangle$. The trace in (3.12) is then proportional to the four-point function

$$W_n(\tau_0, \tau_f; \theta_1, \theta_2) = \left\langle [O^\dagger(w_f)]^n \, \sigma_n(w_2)\sigma_n(w_1) \, [O(w_0)]^n \right\rangle , \tag{3.13}$$

where

$$w_0 = \tau_0 \qquad w_f = \tau_f \qquad w_1 = i\theta_1 \qquad w_2 = i\theta_2. \tag{3.14}$$

Since each of the O's has a 2-twist it becomes necessary to clarify the branching structure of the correlator. Let us specify the indices of the twist fields involved in the correlator:

$$[\sigma_2]^n = \sigma_{(12)}\sigma_{(34)} \cdots \sigma_{(2n-1,2n)} \qquad \sigma_n = \sigma_{(135\ldots 2n-1)}. \tag{3.15}$$

The indices are labels for the $2n$ sheets involved in the correlator, and we use the parenthetical notation for single cycles of S_n. Note that the bare twist σ_n introduced by the replica trick twists one copy from each pair of twisted replicas. This fixes the topology of the correlator.

We can now write the Rényi entanglement entropy as

$$S_n(T, \theta_1, \theta_2) = -\frac{1}{1-n} \log\left(\frac{W_n(-iT-\epsilon, -iT+\epsilon; \theta_1, \theta_2)}{[W_1(-iT-\epsilon, -iT+\epsilon)]^n}\right). \tag{3.16}$$

Note that σ_1 is the identity operator and so there is no need to specify the θ_1 and θ_2 for W_1. Also note that any normalization issues from defining $|\psi_0\rangle$ in terms of the local operator $O(w_0)$ cancel out between the numerator and denominator.

IV. THE FOUR-POINT FUNCTION

The four-point function in Equation (3.13) factorizes into a four-point function of bare twist operators that we compute by mapping to a covering space and a correlator of insertions in the covering space.

We first compute the correlator of the bare twists, and then treat the non-twist supercharge insertions that appear in the covering space. We map the correlator in Equation (3.13) to the plane via the exponential map (2.2). We will then treat the associated Jacobian factors in §IV.4.

IV.1. The twist correlator

Let us begin, then, with just the twist part of the correlator

$$\langle [\sigma_2(z_f)]^n \sigma_n(z_3)\sigma_n(z_2)[\sigma_2(z_0)]^n\rangle\,. \tag{4.1}$$

Note that this part of the correlator applies to any CFT with two copies that are suddenly joined by σ_2. Thus when discussing the bare twist results, we keep c the central charge of a single copy. The SL$(2,\mathbb{C})$ symmetry determines the form of the 4-pt function up to an arbitrary function of the cross-ratio. Therefore, we can compute the 4-pt function

$$\mathcal{F}_n(u) = \langle [\sigma_2(\infty)]^n \sigma_n(u)\sigma_n(1)[\sigma_2(0)]^n\rangle\,, \tag{4.2}$$

and then find the 4-pt function of interest in Equation (4.1).

To compute the four-point function we need to find a map to the covering space, and then compute the Liouville action associated with the map [59]. Fortunately, Appendix D of [51] gives an explicit formula for spherical genus correlation functions of S_N-twist operators as a function of the coefficients of the map. Once we find the map, we can make use of the formula to avoid computing the Liouville action directly.

Let us now list the properties the map $z = z(t)$ from the z-plane to the t-plane must have, as determined by the index structure shown in Equation (3.15). First, one can show from the Riemann–Hurwitz formula that the covering space must have spherical genus:

$$g = \frac{1}{2}\sum_i r_i - s + 1 = \frac{1}{2}[1\cdot n + (n-1) + (n-1) + 1\cdot n] - (2n) + 1 = 0, \tag{4.3}$$

where r_i is the ramification of the ith point with nontrivial monodromy and s is the total number of sheets (or indices) involved. Second, the map must have monodromy at $z = 0$, 1, u, and ∞ appropriate for their respective twist operators. For example, the point $z = 0$ must have n images in the covering space, each with monodromy 2. Third, generic points in the z-plane should have $2n$ distinct images in the t-plane. Thus, we are looking for a meromorphic function $z(t)$ with the following local properties:[2]

$$\begin{aligned}
z &\approx a_j^*(t-t_j^*)^2 && z\approx 0, t\approx t_j^* && j = 0,\ldots,n-1\\
z-1 &\approx a_1 t^n && z\approx 1, t\approx 0 &&\\
z-u &\approx a_u(t-1)^n && z\approx u, t\approx 1 &&\\
z &\approx b_0 t^2 && z\to\infty, t\to t_0^\infty = \infty &&\\
z &\approx \frac{b_j}{(t-t_j^\infty)^2} && z\to\infty, t\approx t_j^\infty && j = 1,\ldots,n-1,
\end{aligned} \tag{4.4}$$

where the a's and b's are coefficients that are determined from the map and the t_j^* and t_j^∞ are the various preimages of $z = 0$ and $z = \infty$, respectively. We have fixed the points 0, 1,

[2] Let us note that in an unfortunate notational choice the stars do *not* indicate complex conjugation. They are merely labels.

and ∞ in the t-plane. The remaining points in the t-plane must be determined from the map.

A rational function that satisfies the above properties is given by

$$z = \left[\frac{At^n - (t-1)^n}{t^n - (t-1)^n}\right]^2, \tag{4.5}$$

where

$$u = A^2. \tag{4.6}$$

Note that

$$t_j^* = \frac{1}{1 - A^{\frac{1}{n}} e^{i\frac{2\pi j}{n}}} \qquad t_j^\infty = \frac{1}{1 - e^{i\frac{2\pi j}{n}}}, \tag{4.7}$$

and we can write

$$\frac{\mathrm{d}z}{\mathrm{d}t} = \frac{2n(A-1)^2}{[t^n - (t-1)^n]^3} t^{n-1}(t-1)^{n-1} \prod_{j=0}^{n-1}(t - t_j^*) \tag{4.8}$$

and

$$t^n - (t-1)^n = n\prod_{j=1}^{n-1}(t - t_j^\infty) \qquad At^n - (t-1)^n = (A-1)\prod_{j=0}^{n-1}(t - t_j^*). \tag{4.9}$$

This allows us to write the map in a form more conducive to finding the a's and b's,

$$z = \frac{(A-1)^2}{n^2} \frac{\prod_{j=0}^{n-1}(t - t_j^*)^2}{\prod_{j=1}^{n-1}(t - t_j^\infty)^2}. \tag{4.10}$$

The coefficients can be written as

$$a_1 = 2(-1)^{n+1}(A-1) \tag{4.11a}$$

$$a_u = 2A(A-1) \tag{4.11b}$$

$$a_k^* = \frac{n(A-1)^2}{[(t_k^*)^n - (t_k^* - 1)^n]^3} (t_k^*)^{n-1}(t_k^* - 1)^{n-1} \prod_{j=0, j\neq k}^{n-1} (t_k^* - t_j^*) \tag{4.11c}$$

$$b_0 = \frac{(A-1)^2}{n^2} \tag{4.11d}$$

$$b_k = \frac{(A-1)^2}{n^2} \left[\frac{\prod_{j=0}^{n-1}(t_k^\infty - t_j^*)}{\prod_{j=1, j\neq k}^{n-1}(t_k^\infty - t_j^\infty)}\right]^2. \tag{4.11e}$$

We can plug these into the formula from [51] to find $\mathcal{F}_n(u)$,

$$\mathcal{F}_n(u) = \left(\prod_{i=1}^{M} p_i^{-\frac{c}{12}(p_i+1)}\right)\left(\prod_{j=0}^{N-1} q_j^{\frac{c}{12}(q_j-1)}\right)\left(\prod_{i=1}^{M} |a_i|^{-\frac{c}{12}\frac{p_i-1}{p_i}}\right)\left(\prod_{j=0}^{F-1} |b_j|^{-\frac{c}{12}\frac{q_j+1}{q_j}}\right)|b_0|^{\frac{c}{6}} q_0^{\frac{c}{6}}, \tag{4.12}$$

where

$$p_j^* \equiv 2 \qquad p_1 = p_w = n \qquad q_j \equiv 2, \tag{4.13}$$

and c is the central charge of a *single* copy of the CFT. (Remember that $c = 6$ for the D1D5 CFT.) All of the various coefficients and products can be checked by appropriate Laurent expansions and by judicious use of the identities (4.9).[3] The final result takes a very simple form

$$\begin{aligned}
\mathcal{F}_n(A) &= \left(2^{-\frac{c}{4}n} n^{-\frac{c}{6}(n+1)}\right)\left(2^{\frac{c}{12}n}\right)\left(\left|4A(A-1)^2\right|^{-\frac{c}{12}\frac{n-1}{n}}\left|n^{2n}\frac{A^{2n-2}}{(A-1)^{2n-4}}\right|^{-\frac{c}{24}}\right) \\
&\quad \times \left|\frac{(A-1)^{2n}}{n^{2n+4}}\right|^{-\frac{c}{8}}\left|\frac{(A-1)^2}{n^2}\right|^{\frac{c}{6}} 2^{\frac{c}{6}} \\
&= \left|4A(A-1)^2\right|^{-\frac{c}{12}\left(n-\frac{1}{n}\right)},
\end{aligned} \tag{4.14}$$

where recall that $A = \sqrt{u}$. As usual, this statement is ambiguous since the square root has two branches. For instance, as one moves u to $z = 1$, A approaches either $+1$ or -1; the amplitude is zero in one case and not in the other. The location of the branch cut plays a crucial role in getting the correct answer, so let us take a moment to discuss its physical origin.

There are two sets of branch cuts associated with the correlator in Equation (4.2). There are the $(12)(34)\cdots$ branch cuts which extend from the origin to infinity, and there is the $(135\cdots)$ branch cut that connects the two σ_n's. From this structure, we see that each of the two σ_n's can be on one of two branches. Physically, then, when u approaches 1 the two σ_n's could be on the same branch and colliding, or they could be on two separate branches and widely separated. This explains the physical origin of the square root.

IV.2. The non-twist insertions

We now include the effect of the non-twist operators. Each application of $G_{-\frac{1}{2}}$ brings in a Jacobian factor when mapped to the covering space. The chiral primary σ_2^{++} inserts an appropriately normalized spin field S^{++} in the covering space [60]; all other Jacobian factors associated with the chiral primary twist operator are taken care of by the Louiville action and the operator normalization.

[3] One needs to plug in with specific values of t and take derivatives to get the desired results.

Thus for each operator inserted at the origin, we write (this is the holomorphic part)

$$\begin{aligned}
\sqrt{2}\left(G^-_{\dot{A},-\frac{1}{2}}\sigma_2^+(0)\right) &= \sqrt{2}\oint_0 \frac{\mathrm{d}z}{2\pi i} G^-_{\dot{A}}(z)\sigma_2^+(0) \\
&\to \sqrt{2}\oint_{t^*} \frac{\mathrm{d}t}{2\pi i}\left(\frac{\mathrm{d}z}{\mathrm{d}t}\right)^{-\frac{1}{2}} G^-_{\dot{A}}(t)\ \left[(a^*)^{-\frac{1}{8}}S^+(t^*)\right] \\
&= \frac{1}{(a^*)^{\frac{5}{8}}}\oint_{t^*}\frac{\mathrm{d}t}{2\pi i}\frac{1}{\sqrt{t-t^*}}\left(\frac{\partial X_{A\dot{A}}(t^*)S^A(t^*)}{\sqrt{t-t^*}}+\dots\right) \\
&= \frac{1}{(a^*)^{\frac{5}{8}}}\partial X_{A\dot{A}}(t^*)S^A(t^*).
\end{aligned} \tag{4.15}$$

The factor of a^* in the square brackets with S^+ is a local normalization that comes with the definition of σ_2^+ [60]. We have suppressed the j index on a^* and t^* in the above. Let us define

$$O_{\dot{A}}(t) = \partial X_{A\dot{A}}(t)S^A(t). \tag{4.16}$$

For the operators inserted at infinity we can write a similar expression; however, it is helpful to make what we mean by "infinity" more precise by making the complex plane into a sphere. Following [59], we cut both the z- and t-planes into large discs with all operators in the finite plane enclosed, and then glue equal-sized discs on top. Then infinity of the original plane becomes a point centered on this "second" disc. The radius of the z-plane discs is $1/\delta$ and the the radius of the t-plane discs is $1/\delta'$.

The insertions at infinity become

$$\left((G^\dagger)^{\dot{A}}_{-,-\frac{1}{2}}\sigma_{2,+}(\infty)\right) \to \delta^{\frac{5}{4}}\, b^{\frac{5}{8}}\, (O^\dagger)^{\dot{A}}(t^\infty), \tag{4.17}$$

where again we have suppressed the index j on b and t^∞. The exception to the above is the $j=0$ insertion at $t_0^\infty = \infty$. This insertion, gets an additional factor of δ':

$$\left((G^\dagger)^{\dot{A}}_{-,-\frac{1}{2}}\sigma_{2,+}(\infty)\right) \to \frac{\delta^{\frac{5}{4}}}{\delta'^{\frac{5}{2}}}\, b^{\frac{5}{8}}\, (O^\dagger)^{\dot{A}}(\tilde{t}=0). \tag{4.18}$$

The above equations were written for just the left part of the operators, but we must also include the right part. Thus, the contribution from the non-twist insertions may be written as

$$\begin{aligned}
&\left|\frac{\prod_j b_j}{\prod_j a_j^*}\right|^{\frac{5}{4}} \frac{\delta^{\frac{5}{2}n}}{\delta'^5} \\
&\quad\times\left\langle :(O^\dagger)^{\dot{A}\dot{B}}(t_0^\infty)(O^\dagger)^{\dot{A}\dot{B}}(t_1^\infty)\cdots(O^\dagger)^{\dot{A}\dot{B}}(t_{n-1}^\infty): :O_{\dot{A}\dot{B}}(t_0^*)\cdots O_{\dot{A}\dot{B}}(t_{n-1}^*):\right\rangle \quad \text{(no sum)},
\end{aligned} \tag{4.19}$$

where the insertion at t_0^∞ should be thought of as at $t = 1/\delta'$ (really at $\tilde{t} = 0$); the end result being that the δ's cancel out in the limit as $\delta' \to 0$. We can evaluate the products of the a^*s and bs as before:

$$\frac{\delta^{\frac{5}{2}n}}{\delta'^5}\left[\frac{|A-1|^{5(n-1)}}{n^{5(n+1)}|A|^{5\frac{n-1}{2}}}\right] \\ \times \left\langle :(O^\dagger)^{\dot{A}\dot{B}}(\infty)(O^\dagger)^{\dot{A}\dot{B}}(t_1^\infty)\cdots(O^\dagger)^{\dot{A}\dot{B}}(t_{n-1}^\infty): :O_{\dot{A}\dot{B}}(t_0^*)\cdots O_{\dot{A}\dot{B}}(t_{n-1}^*):\right\rangle \quad \text{(no sum)}. \tag{4.20}$$

The bracketed expression is the Jacobian factor from the map and the factor of $\delta^{5n/2}$ corresponds to the fact that we have n operators with weight $5/8$ (subtracting off the weight of the bare twist) in the left and right sectors inserted at infinity in the z-plane. Note that the correlator of bare twist operators has a factor of $\delta^{3n/2}$ that has been dropped in (4.12), since we really want the regularized correlator.

Since we are dealing with free fields the above correlator is easily evaluated in terms of Wick contractions. For instance, for $n = 2$ we have

$$\begin{aligned}\frac{1}{\delta'^5}\left\langle :(O^\dagger)^{\dot{A}\dot{B}}(t_0^\infty)(O^\dagger)^{\dot{A}\dot{B}}(t_1^\infty): :O_{\dot{A}\dot{B}}(t_0^*)O_{\dot{A}\dot{B}}(t_1^*):\right\rangle &= \frac{1}{|t_1^\infty - t_0^*|^5} + \frac{1}{|t_1^\infty - t_1^*|^5} \\ &= \left|\frac{1}{2} - \frac{1}{1-\sqrt{A}}\right|^{-5} + \left|\frac{1}{2} - \frac{1}{1+\sqrt{A}}\right|^{-5} \\ &= 2^5\frac{|1-\sqrt{A}|^{10} + |1+\sqrt{A}|^{10}}{|1-A|^5}. \end{aligned} \tag{4.21}$$

Thus putting all of the contributions together for $n = 2$ we find

$$\begin{aligned}\widehat{\mathcal{F}}_2 &= \left|4A(A-1)^2\right|^{-\frac{3}{4}} \cdot \left[\frac{|A-1|^5}{2^{15}|A|^{\frac{5}{2}}}\right] \cdot 2^5\frac{|1-\sqrt{A}|^{10} + |1+\sqrt{A}|^{10}}{|1-A|^5} \\ &= 2^{-\frac{23}{2}}|A|^{-\frac{13}{4}}|A-1|^{-\frac{3}{2}}\left(|1-\sqrt{A}|^{10} + |1+\sqrt{A}|^{10}\right). \end{aligned} \tag{4.22}$$

We use this to find the Rényi entropy of order 2.

Unfortunately, we could not find a closed-form expression for the general covering space amplitude suitable for analytic continuation. It may, however, be written as the sum over all total Wick contractions:

$$\left\langle :(O^\dagger)^{\dot{A}\dot{B}}(\infty)(O^\dagger)^{\dot{A}\dot{B}}(t_1^\infty)\cdots(O^\dagger)^{\dot{A}\dot{B}}(t_{n-1}^\infty): :O_{\dot{A}\dot{B}}(t_0^*)\cdots O_{\dot{A}\dot{B}}(t_{n-1}^*):\right\rangle \\ = \sum_{s\in S_n}\prod_{j=0}^{n-1}|t_{j,s(j)}|^{-5}, \tag{4.23}$$

where $t_{j,k} = t_j^\infty - t_k^*$.

IV.3. The four-point function of interest

We can use (4.14) to find the 4-point function that we actually want. The general form of the 4-point function is dictated by SL$(2, \mathbb{C})$ symmetry to be (cf. [61])

$$A_4 = \langle \phi_4(z_4)\phi_3(z_3)\phi_2(z_2)\phi_1(z_1)\rangle = f(\eta, \bar{\eta}) \prod_{i<j} z_{ij}^{\frac{h}{3}-h_i-h_j} \bar{z}_{ij}^{\frac{\bar{h}}{3}-\bar{h}_i-\bar{h}_j} \qquad \eta = \frac{z_{12}z_{34}}{z_{13}z_{24}}, \tag{4.24}$$

where $z_{ij} = z_i - z_j$ and $f(\eta, \bar{\eta})$ is a function that is completely undetermined by SL$(2, \mathbb{C})$ symmetry. We can compute the 4-point function with points, 0, 1, u, and ∞, and determine f and therefore the general 4-point function.

IV.3.1. The four-point function of bare twists

We separately compute the entanglement entropy of the bare twist operator σ_2 and of the full deformation operator.

In our case the operators are left–right symmetric and therefore $h_i = \bar{h}_i$, and

$$A_4 = f(\eta) \prod_{i<j} |z_{ij}|^{2(\frac{h}{3}-h_i-h_j)}. \tag{4.25}$$

We know that the conformal scaling dimensions for the bare twists are [57, 62]

$$h_1 = h_4 = n\frac{c}{24}\left(2 - \frac{1}{2}\right) \qquad h_2 = h_3 = \frac{c}{24}\left(n - \frac{1}{n}\right), \tag{4.26}$$

Above, we computed the correlator with

$$z_1 = 0 \qquad z_4 = \infty \qquad z_2 = 1 \qquad z_3 = u. \tag{4.27}$$

For this case, we have

$$\eta = \frac{1}{u} \tag{4.28}$$

and thus the 4-point function takes the form

$$A_4 = |\infty|^{-4h_4} \left[f(\eta)|1-u|^{2(\frac{h}{3}-2h_2)}|u|^{2(\frac{h}{3}-h_1-h_2)} \right], \tag{4.29}$$

where we regulated the factor of "∞" by putting the CFT on a disc (see above). We are interested in the finite part.

We can then write the general 4-pt function in terms of the one we computed as (we use the fact that $h_1 = h_4$ and $h_2 = h_3$)

$$A_4 = \mathcal{F}_n(u) \left| \frac{\eta}{1-\eta} z_{23} \right|^{-4h_2} |z_{0f}|^{-4h_1} \qquad u = \frac{1}{\eta}. \tag{4.30}$$

Plugging in with the above weights and with $\mathcal{F}$ from Equation (4.14)

$$\langle \sigma_2(z_f)\sigma_n(z_2)\sigma_n(z_3)\sigma_2(z_0)\rangle = |z_f - z_0|^{-\frac{cn}{4}} \left| \frac{(1+\sqrt{\eta})^4}{16\,\eta\,(z_2 - z_3)^4} \right|^{\frac{c}{24}(n-\frac{1}{n})}, \tag{4.31}$$

where recall

$$\eta = \frac{(z_0 - z_2)(z_3 - z_f)}{(z_0 - z_3)(z_2 - z_f)} \qquad 1 - \eta = \frac{(z_0 - z_f)(z_2 - z_3)}{(z_0 - z_3)(z_2 - z_f)}. \tag{4.32}$$

Note that the amplitude is invariant under interchange of z_2 and z_3 or z_0 and z_f.

IV.3.2. The four-point function with the full deformation operator for $n = 2$

For the full deformation operator the weights are given by

$$h_1 = h_4 = n \qquad h_2 = h_3 = \frac{1}{4}\left(n - \frac{1}{n}\right). \tag{4.33}$$

Plugging in as before, this gives

$$\left\langle [\widehat{O}^\dagger(z_f)]^n \sigma_n(z_3)\sigma_n(z_2)[\widehat{O}(z_0)]^n \right\rangle = \widehat{\mathcal{F}}_n(u) \left| \frac{\eta}{1-\eta} z_{23} \right|^{-(n-\frac{1}{n})} |z_{0f}|^{-4n}, \tag{4.34}$$

where as before we should replace u with $1/\eta$.

For the case $n = 2$, we can plug in with $\widehat{\mathcal{F}}_2$ from Equation (4.22):

$$\left\langle [\widehat{O}^\dagger(z_f)]^2 \sigma_2(z_3)\sigma_2(z_2)[\widehat{O}(z_0)]^2 \right\rangle = 2^{-\frac{23}{2}} |z_{23}|^{-\frac{3}{2}} |z_{0f}|^{-8} \left| \frac{1+\sqrt{\eta}}{\eta^{\frac{1}{4}}} \right|^{\frac{3}{2}} \frac{|1-\eta^{\frac{1}{4}}|^{10} + |1+\eta^{\frac{1}{4}}|^{10}}{|\eta|^{\frac{5}{4}}}. \tag{4.35}$$

We have carefully written the above expression so that the $\eta \mapsto 1/\eta$ symmetry is manifest. This symmetry comes from the exchange symmetry $z_2 \leftrightarrow z_3$ or $z_0 \leftrightarrow z_f$.

IV.4. From the cylinder to the plane

The physics of the D1D5 system originates on the (Lorentzian) cylinder, so we should be careful to put in Jacobian factors that arise in using the exponential map from the cylinder to the plane. Normalized states are normalized states, so we do not need to worry about Jacobian factors for the O_i and $O_i^\dagger$. We do, however, need to worry about Jacobian factors from the replica twists.

We started on the plane with dimensionful coordinates $t \in \mathbb{R}$ and $y \in [0, 2\pi R)$ and then introduced Euclidean dimensionless coordinates τ, θ via (2.1) that may be written as a complex coordinate $w = \tau + i\theta$. Note that R is the radius of the large S^1 cycle that the D1s wrap. Finally, we map to the complex plane using the map in (2.2):

$$\begin{aligned} z &= e^{w} = e^{\tau + i\theta} \to e^{-i\frac{t}{R} + i\frac{y}{R}} \\ \bar{z} &= e^{\bar{w}} = e^{\tau - i\theta} \to e^{-i\frac{t}{R} - i\frac{y}{R}}, \end{aligned} \tag{4.36}$$

where the arrows show how we should analytically continue back to real time at the end of the calculation.

This is a convenient point in the discussion to put in the appropriate normalization so that

$$N \left\langle O^\dagger O \right\rangle = 1 \Longrightarrow N = |z_{0f}|^{4h_1}. \tag{4.37}$$

This is in the z-plane, but as mentioned above, we can put in the normalization on the cylinder or on the z-plane. One can check that the normalization ensures that we insert a normalized state, which means that $W_1 = 1$. Note that this factor cancels out the inverse factor in Equation (4.30). Starting from the cylinder, we can compute the four-point function as

$$\begin{aligned} W_n &= |z_{0f}|^{4h_1} \left\langle O_i^\dagger \sigma_n(w) \sigma_n(w + i\Delta\theta) O_i \right\rangle \\ &= |z_{0f}|^{4h_1} \left| \frac{z}{R} \right|^{4\Delta_n} \left\langle O_i^\dagger \sigma_n(z) \sigma_n(z e^{i\Delta\theta}) O_i \right\rangle \\ &= |z_{0f}|^{4h_1} \left| \frac{z}{R} \right|^{\frac{c}{6}(n - \frac{1}{n})} \left\langle O_i^\dagger \sigma_n(z) \sigma_n(z e^{i\Delta\theta}) O_i \right\rangle . \end{aligned} \tag{4.38}$$

This normalization ensures that $W_1 = 1$ and this will let us easily compute the entanglement entropies. Note that while the Jacobian factor is unity for $n = 1$, it still gives a nontrivial contribution to the von Neumann entropy defined as the limit as $n \to 1$.

V. THE ENTROPY

We now have all of the pieces to discuss the entropy. Let us first treat the Rényi entanglement entropy of the bare twist operator:

$$\begin{aligned} S_n &= \frac{1}{1-n} \log \frac{W_n}{W_1^n} \\ &= \frac{c}{24}\frac{n+1}{n} \log \left[R^4 \frac{|z_2 - z_3|^4}{|z_2|^2 |z_3|^2} \left| \frac{16\eta}{(1+\sqrt{\eta})^4} \right| \right] . \end{aligned} \tag{5.1}$$

Since we have carefully normalized the W_n so that $W_1 = 1$, the von Neumann entropy is

$$S_{\mathrm{vN}} = \lim_{n\to 1} S_n = \frac{c}{12} \log \left[R^4 \frac{|z_2 - z_3|^4}{|z_2|^2 |z_3|^2} \left| \frac{16\eta}{(1+\sqrt{\eta})^4} \right| \right] . \tag{5.2}$$

The limit is trivial only because we already canceled out the $1-n$ in the denominator. We illustrate various properties of this formula in §VI.

Let us also write down the $n=2$ Rényi entropy for the full deformation operator. This is given by

$$S_2 = -\log W_2 = -\log \left[2^{-\frac{23}{2}} R^{-\frac{3}{2}} \frac{|z_2|^{\frac{3}{4}} |z_3|^{\frac{3}{4}}}{|z_{23}|^{\frac{3}{2}}} \left| \frac{1+\sqrt{\eta}}{\eta^{\frac{1}{4}}} \right|^{\frac{3}{2}} \frac{|1-\eta^{\frac{1}{4}}|^{10} + |1+\eta^{\frac{1}{4}}|^{10}}{|\eta|^{\frac{5}{4}}} \right] . \tag{5.3}$$

Recall that the Rényi entropy gives a lower bound for the von Neumann entropy and that it vanishes if and only if the reduced density matrix is that of a pure state.

V.1. Entanglement of the vacuum

It is useful to subtract off the contribution to the entanglement entropy from the vacuum, which we compute here. We want to compute this as a function of the physical cylinder coordinates, so we include Jacobian factors for the map $z \to y$, while keeping the convenient variables $z = e^{iy/R}$. From the above, we have

$$\begin{aligned} S_n^{\mathrm{vac}} &= \frac{1}{1-n} \log \left[\left| \frac{z}{R} \right|^{\frac{c}{6}(n-\frac{1}{n})} \left\langle \sigma_n(z) \sigma_n(z e^{i\theta}) \right\rangle \right] \\ &= \frac{1}{1-n} \log \left[\left| \frac{1}{R} \frac{z_2}{z_2 - z_3} \right|^{\frac{c}{6}(n-\frac{1}{n})} \right] \\ &= \frac{c}{6}\frac{n+1}{n} \log R \left| \frac{z_2 - z_3}{z_2} \right| . \end{aligned} \tag{5.4}$$

The limit as $n \to 1$ yields the von Neumann entropy

$$S_{\rm vN}^{\rm vac} = \frac{c}{3} \log R \left| \frac{z_2 - z_3}{z_2} \right| . \tag{5.5}$$

Since $z_3 = e^{i\theta} z_2$ we have

$$\left| \frac{z_3 - z_2}{z_2} \right| = \left| \frac{z_3}{z_2} - 1 \right| = \left| e^{i\theta} - 1 \right| = 2 |\sin \tfrac{\theta}{2}|, \tag{5.6}$$

and so

$$S_{\rm vN}^{\rm vac} = \frac{c}{3} \log \left[\frac{L}{\pi} \sin \left(\frac{\pi l}{L} \right) \right] , \tag{5.7}$$

where we have written the above expression in terms of $l = |y_2 - y_1|$ and $L = 2\pi R$ to show agreement with [56, 57] for a CFT on a cylinder.

Actually, in the above we have suppressed an ultraviolet cutoff a in terms of which we measure the physical lengths l and L. So the correct expression is (5.7) with l and L replaced by l/a and L/a. There is a logarithmic divergence of $S_{\rm vN}^{\rm vac}$ as $a \to 0$ as noted in early investigations [56, 63]. One can either treat the expression as an asymptotic result for a small but finite a, as would be appropriate for studying lattice theories (e.g., in condensed matter theory), or find "renormalized" entropy *differences* between various states in the theory. In some cases these differences are finite in the $a \to 0$ limit [56].

Here we follow the latter approach (although, as it turns out, our entropy differences are still divergent), since we are interested in the extra entanglement added by the quenching process: the entanglement entropy increase, ΔS. After subtracting off the entanglement of the vacuum we get for the insertions of the bare twist operators

$$\Delta S_{\rm vN} = \frac{c}{12} \log \left| \frac{16\eta}{(1+\sqrt{\eta})^4} \right| \tag{5.8}$$

and similarly for the full deformation operators:

$$\Delta S_2 = \log \left[2^{\frac{23}{2}} \left| \frac{\eta^{\frac{1}{4}}}{1+\sqrt{\eta}} \right|^{\frac{3}{2}} \frac{|\eta|^{\frac{5}{4}}}{|1-\eta^{\frac{1}{4}}|^{10} + |1+\eta^{\frac{1}{4}}|^{10}} \right] . \tag{5.9}$$

VI. PROPERTIES

In this section we include plots of the entropies $\Delta S_{\rm vN}$ and ΔS_2 for a variety of space and time intervals and examine some of their properties. We discuss the details of the

UV cutoff and the choices of branch cuts needed to compute with the entropy formulas we have given. We start with the entanglement entropy introduced by the bare twist operator, then consider the full deformation operator.

VI.1. The entanglement from a bare twist

Our formula (5.8) can now be computed for any time and choice of interval $[\theta_1, \theta_2]$. We recall that the quench is located at $\theta = 0$ and $t = 0$. To actually compute from (5.8) we must choose c, ϵ (as described in §III.1), and a prescription for the square roots (as mentioned at the end of §IV.1). In this subsection, we choose $c = 1$.[4] The entropy increase ΔS diverges as $\epsilon \to 0$ for some values of t, see (6.9) below. We can understand this by thinking of ϵ as a UV suppression factor or regulator, consistent with its appearance in the evolution operator $e^{-iH(t-i\epsilon)}$. It is perhaps not surprising that the local quench has a UV divergence since it is localized at a point, a phenomenon observed in [64]. In a real physical process there should of course be a finite amount of energy, which we can treat as a finite ϵ in our calculation. We would fix the appropriate value of ϵ in a full treatment of the physical evolution of the D1D5 CFT, but here we leave it as an unfixed but small parameter. With finite ϵ we have

$$\begin{aligned} \eta &= \frac{\sin\left(\frac{1}{2}(\frac{t}{R} + \theta_1 - i\epsilon)\right) \sin\left(\frac{1}{2}(\frac{t}{R} + \theta_2 + i\epsilon)\right)}{\sin\left(\frac{1}{2}(\frac{t}{R} + \theta_1 + i\epsilon)\right) \sin\left(\frac{1}{2}(\frac{t}{R} + \theta_2 - i\epsilon)\right)}, \\ \bar{\eta} &= \frac{\sin\left(\frac{1}{2}(\frac{t}{R} - \theta_1 - i\epsilon)\right) \sin\left(\frac{1}{2}(\frac{t}{R} - \theta_2 + i\epsilon)\right)}{\sin\left(\frac{1}{2}(\frac{t}{R} - \theta_1 + i\epsilon)\right) \sin\left(\frac{1}{2}(\frac{t}{R} - \theta_2 - i\epsilon)\right)} \end{aligned} \tag{6.1}$$

where here $\theta_i = y_i/R$ and ϵ should really be ϵ/R so that all parameters are dimensionless. For the remainder of our discussion, we set $R = 1$. In the above expressions and in what follows, θ parametrizes the double circle by running from $\theta = 0$ to $\theta = 4\pi$. This explains the factors of $1/2$ inside the trigonometric functions.

Using sundry trigonometric identities, we can rewrite η and $\bar{\eta}$ in a slightly more useful form

$$\eta = e^{2i\varphi} \qquad \tan\varphi = \tilde{\epsilon}\frac{\cot\frac{t+\theta_2}{2} - \cot\frac{t+\theta_1}{2}}{1 + \tilde{\epsilon}^2 \cot\frac{t+\theta_2}{2}\cot\frac{t+\theta_1}{2}}, \tag{6.2}$$

[4] The appropriate choice for the D1D5 CFT would be $c = 6$; however, the c-dependence is just an overall constant here, and since the bare twist operator is not the deformation operator, we may as well just set $c = 1$.

where we have introduced $\tilde{\epsilon} = \tanh(\epsilon/2)$. For our purposes, it suffices to drop the $\tilde{\epsilon}^2$ term in the denominator and write

$$\tan\varphi \approx \tilde{\epsilon}\left[\cot\tfrac{t+\theta_2}{2} - \cot\tfrac{t+\theta_1}{2}\right] \approx 0^{\pm} \Longrightarrow \varphi \approx n\pi \qquad n \in \mathbb{Z}. \tag{6.3}$$

From the above, we conclude that for small ϵ φ is close to some multiple of π, and therefore η is essentially unity. This fact could have been read off from (6.1) directly; the key realization from the above is that the *sign* of the 0 depends on time which implies φ has some nontrivial time-dependence. If we plot φ as function of t for reasonably small ϵ and take care with the signs, we get Figure 3. Note that $\tan\varphi$ never vanishes in (6.2), and therefore $-\pi < \varphi < 0$. We have chosen these particular branches to be consistent with (6.4).

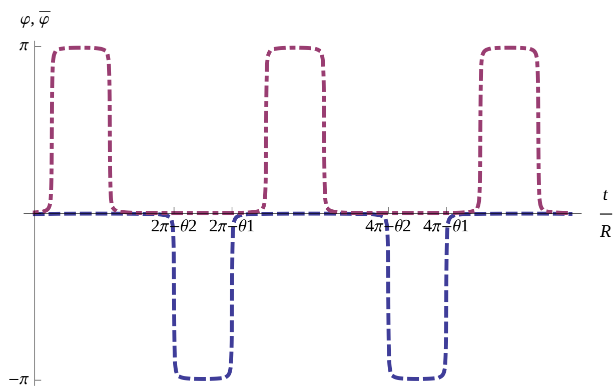

FIG. 3. (color online) Plot of φ (blue, dashed) and $\bar{\varphi}$ (red, dot-dashed) versus time for $\epsilon = 10^{-2}$, where $\eta = \exp 2i\varphi$ and $\bar{\eta} = \exp 2i\bar{\varphi}$. Note that φ and $\bar{\varphi}$ obey the strict inequality $-\pi < \varphi < 0 < \bar{\varphi} < \pi$ for all time. In the limit as ϵ goes to zero, the function converges pointwise to a piecewise function saturating the inequalities. Indeed, for $\epsilon = 10^{-4}$ the plot is (visually) indistinguishable from the corresponding piecewise function.

All of the time dependence comes from the interaction of this phase with the square root. We have carefully chosen φ and $\bar{\varphi}$ in Figure 3 so that the correct branches are

$$\sqrt{\eta} = e^{i\varphi} \qquad \sqrt{\bar{\eta}} = e^{i\bar{\varphi}} \qquad \eta^{\frac{1}{4}} = -e^{i\frac{\varphi}{2}} \qquad \bar{\eta}^{\frac{1}{4}} = -e^{i\frac{\bar{\varphi}}{2}}, \tag{6.4}$$

where the fourth roots arise when considering the Rényi entropy of the full deformation operator. Then, we can write the entropy in terms of φ and $\bar{\varphi}$

$$\Delta S_{\mathrm{vN}} = -\frac{c}{6}\log\left(\cos\tfrac{1}{2}\varphi\right) - \frac{c}{6}\log\left(\cos\tfrac{1}{2}\bar{\varphi}\right) \tag{6.5}$$

Note that in defining φ and $\bar{\varphi}$ from (6.2) there is an ambiguity associated $\tan$; similarly, in writing the square root of η in terms of φ and $\bar{\varphi}$ there are two branches one could choose. However, the above choices are fixed for us by casuality: the entanglement entropy of our interval cannot change from the vacuum value until a signal traveling at the speed of light from the quench could reach the interval. The origin of the branch cut is also discussed at the end of §IV.1.

Since for small ϵ, φ and $\bar{\varphi}$ spend the vast majority of time near 0 or $\pm\pi$, let us examine the limiting behavior of the entropy away from the transitions. This is where the approximations in Equation (6.3) are good. Let us define x to be the difference of cotangents,

$$x = \cot\tfrac{t+\theta_2}{2} - \cot\tfrac{t+\theta_1}{2}. \tag{6.6}$$

Then, for small $\tilde{\epsilon}x$ we can write

$$\cos^2\frac{\varphi}{2} \approx \begin{cases} 1 - \frac{1}{4}(\tilde{\epsilon}x)^2 + O\big((\tilde{\epsilon}x)^4\big) & x<0 \\ \frac{1}{4}(\tilde{\epsilon}x)^2 + O\big((\tilde{\epsilon}x)^4\big) & x>0 \end{cases}, \tag{6.7}$$

and thus the left-moving contribution to the entanglement entropy is given by

$$S_L = -\log\big(\cos\tfrac{\varphi}{2}\big) \approx \begin{cases} \frac{1}{8}(\tilde{\epsilon}x)^2 + O\big((\tilde{\epsilon}x)^4\big) & x<0 \\ -\log\frac{1}{2}\tilde{\epsilon}x + O\big((\tilde{\epsilon}x)^2\big) & x>0 \end{cases}. \tag{6.8}$$

We see that the entanglement entropy (away from transition regions) either vanishes like $\tilde{\epsilon}^2$ or diverges like $-\log\tilde{\epsilon}$. The peak value occurs at $t = -\frac{\theta_1+\theta_2}{2} + 2n\pi$ for integer n. We can estimate the peak value as

$$S_L^{\text{peak}} \approx -\log\tilde{\epsilon} + \log\big(\tan\tfrac{\theta_2-\theta_1}{4}\big) + O(\tilde{\epsilon}^2). \tag{6.9}$$

The unbounded growth of S_L^{peak} as $\epsilon \to 0$ indicates that the state after the local quench has entangled elements of arbitrarily high energy, a UV effect already discussed.

The ϵ dependence of S_L^{peak} indicates only partial thermalization, as we now discuss. We can think of the UV regulator ϵ as introducing a temperature $1/2\epsilon$, in that it corresponds to introducing the operator $e^{-2\epsilon H}$ in our density matrix given in (3.4). We can compare the ϵ dependence of S_L^{peak} with the entanglement entropy of the interval in the equilibrium mixed state at temperature $1/2\epsilon$. The limit $\epsilon \to 0$ corresponds to high temperatures and in this limit the entropy should be dominated by the extensive quantity

$$S_L^{\text{max}}\Big|_{\epsilon\to 0} \sim \frac{\Delta\theta}{\epsilon}. \tag{6.10}$$

This gives the asymptotic behavior of a general CFT of length $\Delta\theta$ at temperature $1/\epsilon$, which is a regularized expression for the maximum entropy on that interval. Thus, we see that while the entanglement entropy we produce diverges, it is parametrically less than the maximum possible entropy for the subsystem. In other words, even at peak entanglement, the system is far from being "Page-scrambled" as defined in [14], referring to [65]. This is expected since being Page-scrambled would require the reduced density matrix after the quench to evolve to the maximal-entropy (infinite-temperature) thermal density matrix, proportional to the identity operator on $\mathcal{H}_A$, but we do not expect a local quench to lead to a thermal reduced density matrix (at any temperature). Firstly, this system has decoupled momentum sectors which can thus be independently thermalized with various momentum-dependent temperatures [11]. Secondly, the local quench produces coherent sets of non-interacting particles traveling from the quench point, so there is no mechanism to scramble their momenta. So thermalization must involve more than the process we study here, as we discuss further in the Conclusion.

Now we can examine some specific calculations of ΔS_{vN}, choosing $c = 1$ and $\epsilon = 10^{-4}$. The branch cuts are chosen as discussed above. The first obvious feature from the formulae is that the entropy is 2π-periodic, which follows from the 2π-periodicity of the quenching process; the point where the two circles join becomes two anti-podal points on the length $4\pi R$ circle.

In figure 4a we choose the interval $[\pi/2, 3\pi/4]$ and see positive entropy at those times when the null world line from the quench point intersects the interval. We have separated the contribution from the left-moving and right-moving sectors for illustrative purposes. With the interval to the right of the quench point, the the entropy can be qualitatively understood in terms of particles emitted from the quench point and traveling with unit velocity, a picture first described in [52]. The positive entropy comes from the presence of entangled pairs of (left- or right-moving) particles, one member of which is inside the interval and the other outside, and so is traced over. A space-time picture of this is given in Figure 5 and we discuss it further in the Conclusion. ΔS_2 behaves the same way, as shown in Figure 4b. In fact, plots of ΔS_2 take almost exactly the same shapes and share all the qualitative properties of those of ΔS_{vN}, so we only include plots of the latter in the following.

We can translate the interval toward and away from the quench point, as seen in Fig-

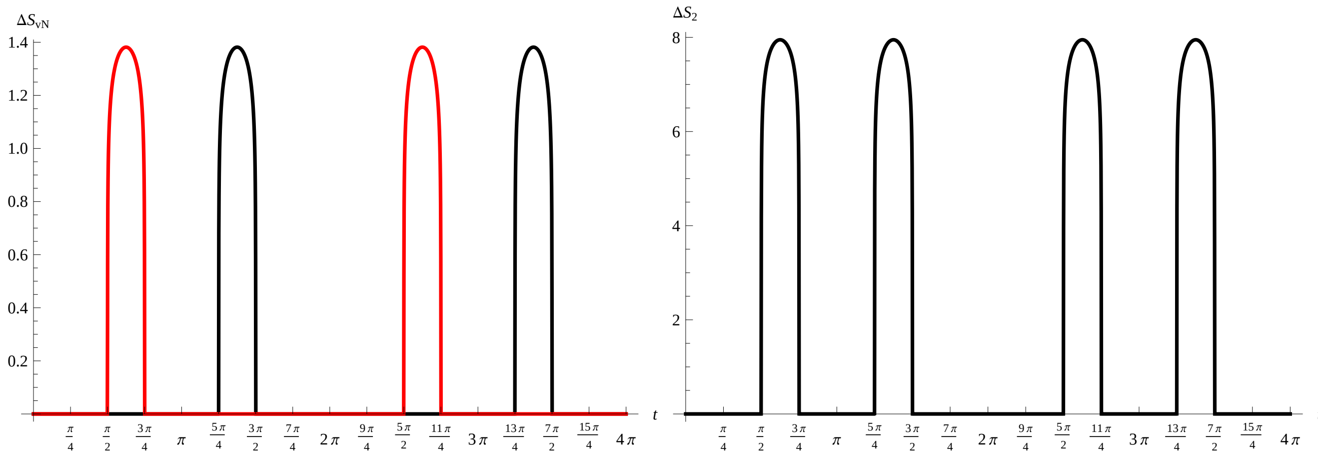

(a) (b)

FIG. 4. (color online) ΔS_{vN}, 4a, and ΔS_2, 4b, for the interval $[\pi/2, 3\pi/4]$. For ΔS_{vN} the right-moving contribution is shown in red (gray), the left-moving in black. For ΔS_2 we cannot separate the left and right-moving contributions.

ure 6a, which is seen to have almost no effect on the entropy curve. However, if the quench takes place inside the interval there is a very noticeable effect shown in Figure 6b, due to overlapping contributions from the left and right-moving sectors. We can examine intervals of different sizes, as in Figure 7, and see a clear dependence on the size of the interval. The dependence of the peak value on the size can be read from the second term in (6.9).

VI.2. The entanglement from the deformation operator

Here we examine the second Rényi entropy that results from quenching with the full deformation operator. The expression for S_2 in (5.3) may be written as

$$S_2 = S_2^{\mathrm{vac}} + S_2^{\mathrm{bare}} + S_2^{\mathrm{ins}}, \tag{6.11}$$

where S_2^{vac} is the Rényi entropy of the vacuum in (5.4), S_2^{bare} is the additional Rényi entropy added by the bare twist in (5.1), and S_2^{ins} is the new contribution from the super-

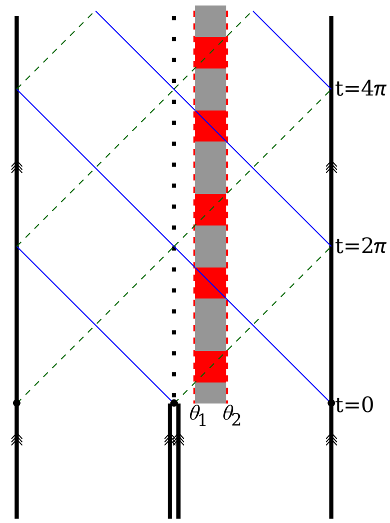

FIG. 5. (color online) Here we show the two circles being joined at $\theta = 0$ and $\theta = 2\pi$. Time is increasing up on the figure. The quench occurs at $t = 0$. Lightcones are emanating from the two quench sites. The right-moving excitations travel along the green (dashed) diagonal lines, and the left-moving excitations along the blue (solid) diagonal lines. The gray vertical strip represents the time-evolution of the interval $[\theta_1, \theta_2]$, and the red (dark) parts of the strip show when we expect nonvanishing entanglement from the particle interpretation.

charge and spin field in the covering space. We write the three pieces as

$$S_2^{\text{vac}} = \frac{3}{4}\log\left|R^2\frac{z_{23}^2}{z_2 z_3}\right| \tag{6.12a}$$

$$S_2^{\text{bare}} = \frac{3}{8}\log\frac{16|\eta|}{|1+\sqrt{\eta}|^4} \tag{6.12b}$$

$$S_2^{\text{ins}} = -\log\frac{|1-\eta^{\frac{1}{4}}|^{10}+|1+\eta^{\frac{1}{4}}|^{10}}{2^{10}|\eta|^{\frac{5}{4}}}. \tag{6.12c}$$

Using (6.4), we can rewrite the last two terms as

$$S_2^{\text{bare}} = -\frac{3}{4}\log\left(\cos\tfrac{\varphi}{2}\right) - \frac{3}{4}\log\left(\cos\tfrac{\bar{\varphi}}{2}\right) \tag{6.13a}$$

$$S_2^{\text{ins}} = -\log\left[\cos^5\tfrac{\varphi}{4}\cos^5\tfrac{\bar{\varphi}}{4} - \sin^5\tfrac{\varphi}{4}\sin^5\tfrac{\bar{\varphi}}{4}\right], \tag{6.13b}$$

and $\Delta S_2 = S_2^{\text{bare}} + S_2^{\text{ins}}$. We plot this for the interval $[\pi/2, 3\pi/4]$ in Figure 4b and, as mentioned, plots analogous to those in Figures 6a, 6b, and 7 look very similar. Let us note that S_2^{ins} is distinguished from the entanglement of the vacuum and of the bare twist in that the left and right contributions do not directly factorize. That being said, one finds that

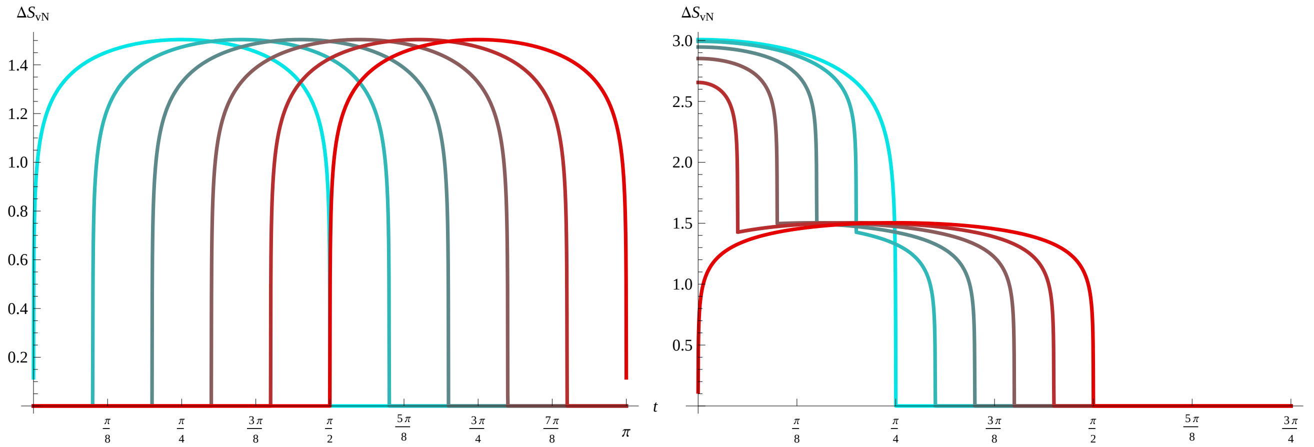

(a) (b)

FIG. 6. (color online) $\Delta S_{\rm vN}$ for various translated equal-size intervals $[0 + x\pi/10, \pi/2 + x\pi/10]$, 6a, and $[-\pi/4 + x\pi/20, \pi/4 + x\pi/20]$, 6b, with the different colors, going from blue-green to red (light to dark), showing $x = 0, 1, 2, 3, 4, 5$.

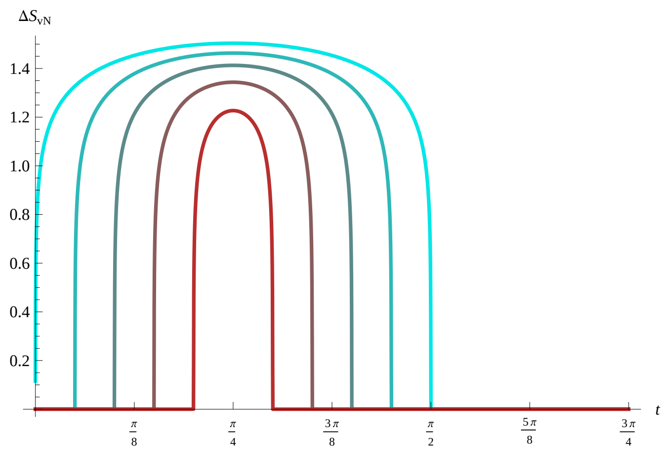

FIG. 7. (color online) $\Delta S_{\rm vN}$ for intervals of various sizes $[\pi/4 - x\pi/20, \pi/2 + x\pi/20]$, with the different colors, going from red to blue-green (dark to light), showing $x = 1, 2, 3, 4, 5$.

$S^{\rm ins}$ still enjoys a superposition principle with respect to the left and right contributions *as long as left- and right-moving excitations do not simultaneously contribute to the entropy.*

To illustrate consider $S_2^{\rm ins}$ in the limit of vanishing ϵ. In particular, the peak value of $S_2^{\rm ins}$ when left or right excitations are separately in the interval is given by

$$\lim_{\epsilon\to 0} S_2^{\rm ins}\Big|_{\text{sing. cont.}} = \frac{5}{2}\log 2, \tag{6.14}$$

and is *finite*. When both left and right excitations contribute, however, S_2^{ins} is given by

$$\lim_{\epsilon\to 0} S_2^{\text{ins}}\bigg|_{\text{both cont.}} = 4\log 2, \tag{6.15}$$

which serves as a finite upper bound on S_2^{ins}; however, it is *not* simply twice the contribution from left- or right-movers separately. Aside from the failure of left and right contributions to factorize, S_2^{ins} is further distinguished in its finiteness. In contrast, S_2^{bare} represents a huge (actually divergent) amount of entanglement. This suggests that it is the twisting part of the deformation operator that predominantly contributes to thermalization. This is consistent with the point of view advocated in [36–38], which focuses on the effect of the twist operator.

VII. CONCLUSION

We have seen how to analytically compute entanglement entropies for arbitrary spatial intervals of the D1D5 CFT following a local quench of the system by an exactly marginal deformation operator, which contains the 2-twist operator and moves the theory toward the supergravity regime in its moduli space. For the insertions of the bare twist operators we were able to compute all of the Rényi entropies S_n and the von Neumann entropy while for the full deformation operators we were only able to compute the S_n for $n \geq 2$. We could understand the qualitative behavior of the entropies as arising from pairs of entangled particles generated at the quench event and propagating from there at the speed of light.

This process does not lead to thermalization of the system, as we saw in the discussion below (6.9), but from the point of the view of the interval these particles should appear as thermal radiation in accord with their non-zero entropy. The non-zero entropy does not itself, of course, guarantee the radiation is thermal, but we expect it is for several reasons. First we note that *global* quenches, which can also be understood as producing pairs of entangled particles [52], do generally lead to thermalized systems [10, 11, 50]. In our case of a local quench, the positive entanglement entropy is apparently due to the entanglement of pairs of localized excitations, one member of which is inside the interval and one outside, and so is traced over. This is a situation familiar from Hawking radiation: it appears thermal to observers outside the horizon.

A toy model illustrates this in more detail. Consider two harmonic oscillators with operators $\{a, a^\dagger\}$ and $\{b, b^\dagger\}$ in the entangled state $|\psi\rangle \propto e^{\lambda a^\dagger b^\dagger}|0\rangle$. Such a squeezed state is the general result of a Bogolyubuv transformation on the operator algebras and appears in our case as (3.1) above. If we then trace over, say, the b oscillator then the resulting reduced density matrix is given by

$$\rho_a \propto \sum_n |\lambda|^{2n} |n\rangle_a \langle n|_a. \tag{7.1}$$

Now we can compare to a thermal density matrix for the a oscillator using (1.1):

$$\rho_{\text{th}} \propto e^{-\beta H_a} \propto \sum_n e^{-\beta\omega n}|n\rangle_a\langle n|_a, \tag{7.2}$$

and we see that ρ_a is a thermal density matrix at inverse temperature $\beta = -\frac{1}{\omega}\log|\lambda|^2$. It is straightforward to compute the entropies of the state ρ_a as a function of λ (or equivalently β) but we do not need the explicit formulas here.

This simple calculation illustrates how thermal density matrices, with their associated entropies, arise from the process we are considering. Of course, the trace we perform in the CFT, over the exterior of a spatial interval, is not directly analogous to this simple case. It seems to be difficult to perform such a spatial trace directly on the state after the quench, given by (3.1), which is why we pursued a technique here that makes extensive use of the powerful conformal symmetry of the system. It would be interesting to pursue that direct approach and also to trace over different classes of subsystems, corresponding to different coarse-grainings.

Ultimately we would like to understand thermalization in this system, with general subsystems characterized by reduced density matrices of the kind in (1.1). Here we have only studied an individual event involving a small sector of the full theory, which is a system of N_1 D1 and N_5 D5 branes with N_1 and N_5 potentially large. This has been in the spirit of time-dependent perturbation theory of a weakly interacting system: individual interactions are treated separately and the cumulative effect of many independent interactions is put together at the end. We can imagine how the thermal radiation produced by many independent local quenches can ultimately lead to a thermalized system, but a full, careful treatment remains to be done.

We would like to compare the entropies produced from such a process to those of the system in equilibrium at some finite temperature, not just the high-temperature limit we considered above. Computing the finite-temperature entropies would involve computing two-point functions of twist operators in a domain with both space and time periodically identified, i.e., a torus. This is somewhat challenging as the answer would depend on the full operator content [61] and one cannot uniformize to the plane. It has been carried out for a single fermion [66] and we hope to address this for the D1D5 system in future work. It should also be possible to learn more information about the state after the quench by judiciously studying the whole set of Rényi entropies that can be obtained from (4.20) and (4.23) (or (5.1) for the bare twists), rather than just $n = 1$ or 2 as we did here, since they collectively contain significantly more information. Our results (particularly for the bare, non-supersymmetric twist operators) may be relevant to and possibly subject to verification by the local quenches studied in condensed matter systems, e.g., [67–69]. However, there a number of issues in making such a comparison, since our CFT and local quench are both highly specific, and we have not seriously attempted to do so.

Finally, a few words on the bulk description of the process we studied. The D1-branes are wrapped in the D5-branes, which are localized in the transverse asymptotically 4+1 dimensional Minkowski space. Initially the branes are in a stationary state corresponding to the ground state of the D1D5 orbifold CFT. We then imagine a sudden interaction with an external field in the transverse space, which weakly deforms the D1D5 system by the exactly marginal twist operator (2.4) and generates excitations that propagate periodically in the AdS throat region. As we discussed in the introduction, dynamics of this sort have been investigated in the supergravity regime [48, 49]. This supplies the energy necessary for thermalization, which would occur after further interactions. This is admittedly just a sketch that we hope to improve.

ACKNOWLEDGMENTS

We thank Tom Faulkner, Joe Polchinski, and Mark Srednicki for helpful discussions. CA thanks David Berenstein, Idse Heemskerk, Gary Horowitz, SungBin Lee, Don Marolf and Emil Martinec and SA thanks Borun Chowdhury, Suresh Govindarajan, Kalyana Rama, Balachandran Sathiapalan, Masaki Shigemori, and Nemani Suryanarayana for conversations and suggestions related to this project. CA is supported in part by the DOE under grant DE-FG02-91ER40618. This research was supported in part by the National Science Foundation under Grant No. NSF PHY05-51164. SA is grateful for the hospitality and support of the KITP, where much of this research was performed.

---

[1] J. M. Maldacena, Adv. Theor. Math. Phys. **2**, 231 (1998), arXiv:hep-th/9711200.

[2] S. N. Solodukhin, Living Rev. Relativity **14**, 8 (2011) arXiv:1104.3712 [hep-th].

[3] S. Lloyd, Nature Phys. **2**, 727 (2006).

[4] J. M. Deutsch, Phys. Rev. A **43**, 2046 (Feb. 1991).

[5] M. Srednicki, Phys. Rev. E **50**, 888 (1994), arXiv:cond-mat/9403051v2.

[6] S. Popescu, A. J. Short, and A. Winter, Nature Phys. **2**, 754 (Nov. 2006), arXiv:quant-ph/0511225v3.

[7] M. Gell-Mann and J.B. Hartle, Phys. Rev. A **76**, 022104 (2007), arXiv:quant-ph/0609190v3.

[8] M. Rigol, V. Dunjko, V. Yurovsky, and M. Olshanii, Phys. Rev. Lett. **98**, 050405 (2007), arXiv:cond-mat/0604476v2.

[9] M. Rigol, V. Dunjko, and M. Olshanii, Nature **452**, 854 (Apr. 2008), arXiv:0708.1324v2 [cond-mat.stat-mech].

[10] M. Rigol and M. Srednicki(2011), arXiv:1108.0928 [cond-mat.stat-mech].

[11] P. Calabrese and J. Cardy, J. Stat. Mech. **0706**, P06008 (2007), arXiv:0704.1880 [cond-mat.stat-mech].

[12] L. Susskind and J. Lindesay, *An Introduction To Black Holes, Information And The String Theory Revolution: The Holographic Universe* (World Scientific Publishing Company, 2004).

[13] *Entanglement Entropy in Extended Quantum Systems*, J. Phys. A, Vol. 42 No. 50 (2009).

[14] Y. Sekino and L. Susskind, J. High Energy Phys. **0810**, 065 (2008), arXiv:0808.2096 [hep-th].

[15] S. R. Das, T. Nishioka, and T. Takayanagi, J. High Energy Phys. **07**, 071 (2010), arXiv:1005.3348 [hep-th].

[16] U. H. Danielsson, E. Keski-Vakkuri, and M. Kruczenski, J. High Energy Phys. **0002**, 039 (2000), arXiv:hep-th/9912209v2.

[17] S. B. Giddings and A. Nudelman, J. High Energy Phys. **0202**, 003 (2002), arXiv:hep-th/0112099.

[18] P. M. Chesler and L. G. Yaffe, Phys. Rev. Lett. **102**, 211601 (2009), arXiv:0812.2053 [hep-th].

[19] S. Bhattacharyya and S. Minwalla, J. High Energy Phys. **0909**, 034 (2009), arXiv:0904.0464

[hep-th].

[20] C. T. Asplund and D. Berenstein, Phys. Lett. **B673**, 264 (2009), arXiv:0809.0712 [hep-th].

[21] V. E. Hubeny and M. Rangamani, Adv. High Energy Phys. **2010**, 297916 (2010), arXiv:1006.3675 [hep-th].

[22] V. Balasubramanian, A. Bernamonti, J. de Boer, N. Copland, B. Craps, *et al.*, Phys. Rev. Lett. **106**, 191601 (2011), arXiv:1012.4753 [hep-th].

[23] V. Balasubramanian, A. Bernamonti, J. de Boer, N. Copland, B. Craps, E. Keski-Vakkuri, B. Müller, A. Schäfer, M. Shigemori, and W. Staessens, Phys. Rev. D **84**, 026010 (Jul. 2011), arXiv:1103.2683 [hep-th].

[24] T. Albash and C. V. Johnson, New J. Phys. **13**, 045017 (2011), arXiv:1008.3027 [hep-th].

[25] J. Abajo-Arrastia, J. a. Aparício, and E. López, J. High Energy Phys. **1011**, 149 (2010), arXiv:1006.4090 [hep-th].

[26] S. Ryu and T. Takayanagi, Phys. Rev. Lett. **96**, 181602 (2006), arXiv:hep-th/0603001.

[27] V. E. Hubeny, M. Rangamani, and T. Takayanagi, J. High Energy Phys. **0707**, 062 (2007), arXiv:0705.0016 [hep-th].

[28] M. Headrick, Phys. Rev. D **82**, 126010 (2010), arXiv:1006.0047 [hep-th].

[29] A. Strominger and C. Vafa, Phys. Lett. **B379**, 99 (1996), arXiv:hep-th/9601029.

[30] C. G. Callan and J. M. Maldacena, Nucl. Phys. **B472**, 591 (1996), arXiv:hep-th/9602043.

[31] B. D. Chowdhury and S. D. Mathur, Class. Quant. Grav. **25**, 135005 (2008), arXiv:0711.4817 [hep-th].

[32] B. D. Chowdhury and S. D. Mathur, Class. Quant. Grav. **25**, 225021 (2008), arXiv:0806.2309 [hep-th].

[33] B. D. Chowdhury and S. D. Mathur, Class. Quant. Grav. **26**, 035006 (2009), arXiv:0810.2951 [hep-th].

[34] S. G. Avery, B. D. Chowdhury, and S. D. Mathur, J. High Energy Phys. **0910**, 065 (2009), arXiv:0906.2015 [hep-th].

[35] S. G. Avery and B. D. Chowdhury, J. High Energy Phys. **1001**, 087 (2010), arXiv:0907.1663 [hep-th].

[36] S. G. Avery, B. D. Chowdhury, and S. D. Mathur, J. High Energy Phys. **1006**, 031 (2010), arXiv:1002.3132 [hep-th].

[37] S. G. Avery, B. D. Chowdhury, and S. D. Mathur, J. High Energy Phys. **1006**, 032 (2010),

arXiv:1003.2746 [hep-th].

[38] S. G. Avery and B. D. Chowdhury, J. High Energy Phys. **1105**, 025 (2011), arXiv:1007.2202 [hep-th].

[39] E. Gava and K. Narain, J. High Energy Phys. **0212**, 023 (2002), arXiv:hep-th/0208081.

[40] A. Pakman, L. Rastelli, and S. S. Razamat, J. High Energy Phys. **1005**, 099 (2010), arXiv:0912.0959 [hep-th].

[41] S. R. Das and S. D. Mathur, Nucl. Phys. **B478**, 561 (1996), arXiv:hep-th/9606185.

[42] D. Birmingham, I. Sachs, and S. N. Solodukhin, Phys. Rev. Lett. **88**, 151301 (2002), arXiv:hep-th/0112055v2.

[43] D. Birmingham, I. Sachs, and S. N. Solodukhin, Phys. Rev. D **67**, 104026 (2003), arXiv:hep-th/0212308.

[44] I. Bena, B. D. Chowdhury, J. de Boer, S. El-Showk, and M. Shigemori(2011), arXiv:1108.0411 [hep-th].

[45] G. Festuccia and H. Liu, J. High Energy Phys. **0712**, 027 (2007), arXiv:hep-th/0611098.

[46] N. Iizuka and J. Polchinski, J. High Energy Phys. **0810**, 028 (2008), arXiv:0801.3657 [hep-th].

[47] N. Iizuka, T. Okuda, and J. Polchinski, J. High Energy Phys. **1002**, 073 (2010), arXiv:0808.0530 [hep-th].

[48] O. Lunin and S. D. Mathur, Nucl. Phys. **B615**, 285 (2001), arXiv:hep-th/0107113 [hep-th].

[49] S. Giusto, S. D. Mathur, and A. Saxena, Nucl. Phys. **B710**, 425 (2005), arXiv:hep-th/0406103 [hep-th].

[50] T. Takayanagi and T. Ugajin, J. High Energy Phys. **1011**, 054 (2010), arXiv:1008.3439 [hep-th].

[51] S. Avery, *Using the D1D5 CFT to Understand Black Holes*, Ph.D. thesis, Ohio State Univ. (Nov. 2010), arXiv:1012.0072 [hep-th].

[52] P. Calabrese and J. L. Cardy, J. Stat. Mech. **0504**, P04010 (2005), arXiv:cond-mat/0503393.

[53] P. Calabrese and J. Cardy, J. Stat. Mech. **2007**, P10004 (2007), arXiv:0708.3750v2 [cond-mat].

[54] W. Ochs, Rep. Mathematical Phys. **8**, 109 (Aug. 1975).

[55] J. Callan, Curtis G. and F. Wilczek, Phys.Lett. **B333**, 55 (1994), arXiv:hep-th/9401072.

[56] C. Holzhey, F. Larsen, and F. Wilczek, Nucl. Phys. **B424**, 443 (1994), arXiv:hep-th/9403108.

[57] P. Calabrese and J. L. Cardy, J. Stat. Mech. **0406**, P06002 (2004), arXiv:hep-th/0405152v3.

[58] E. A. Calzetta and B. B. Hu, *Nonequilibrium Quantum Field Theory* (Cambridge University Press, 2008).

[59] O. Lunin and S. D. Mathur, Commun. Math. Phys. **219**, 399 (2001), arXiv:hep-th/0006196.

[60] O. Lunin and S. D. Mathur, Commun. Math. Phys. **227**, 385 (2002), arXiv:hep-th/0103169.

[61] P. DiFrancesco, P. Mathieu, and D. Senechal, *Conformal Field Theory*, corr. 2nd print. ed. (Springer, New York, 1999).

[62] V. Knizhnik, Commun. Math. Phys. **112**, 567 (1987).

[63] M. Srednicki, Phys. Rev. Lett. **71**, 666 (1993), arXiv:hep-th/9303048.

[64] A. Anderson and B. DeWitt, Found. Phys. **16**, 91 (Feb. 1986).

[65] D. N. Page, Phys. Rev. Lett. **71**, 1291 (1993), arXiv:gr-qc/9305007.

[66] T. Azeyanagi, T. Nishioka, and T. Takayanagi, Phys. Rev. D **77**, 064005 (2008), arXiv:0710.2956v4 [hep-th].

[67] V. Eisler and I. Peschel, J. Stat. Mech. **6**, 06005 (2007), arXiv:cond-mat/0703379v3.

[68] F. Iglói, Z. Szatmári, and Y.-C. Lin, Phys. Rev. B **80**, 024405 (Jul. 2009), arXiv:0903.3740v1 [cond-mat.stat-mech].

[69] B. Hsu, E. Grosfeld, and E. Fradkin, Phys. Rev. B **80**, 235412 (2009), arXiv:0908.2622v2 [cond-mat.mes-hall]

.